



Webster, R. F., Cherns, D., Novikov, S. V., & Foxon, C. T. (2014). Transmission electron microscopy of indium gallium nitride nanorods grown by molecular beam epitaxy. *Physica Status Solidi C-Current Topics in Solid State Physics*, 11(3-4), 417-420. 10.1002/pssc.201300454

Link to published version (if available):  
[10.1002/pssc.201300454](http://10.1002/pssc.201300454)

[Link to publication record in Explore Bristol Research](#)  
PDF-document

## University of Bristol - Explore Bristol Research

### General rights

This document is made available in accordance with publisher policies. Please cite only the published version using the reference above. Full terms of use are available:  
<http://www.bristol.ac.uk/pure/about/ebr-terms.html>

### Take down policy

Explore Bristol Research is a digital archive and the intention is that deposited content should not be removed. However, if you believe that this version of the work breaches copyright law please contact [open-access@bristol.ac.uk](mailto:open-access@bristol.ac.uk) and include the following information in your message:

- Your contact details
- Bibliographic details for the item, including a URL
- An outline of the nature of the complaint

On receipt of your message the Open Access Team will immediately investigate your claim, make an initial judgement of the validity of the claim and, where appropriate, withdraw the item in question from public view.

# Transmission electron microscopy of Indium Gallium Nitride nanorods grown by molecular beam epitaxy

Richard F Webster<sup>\*1</sup>, David Cherns<sup>1</sup>, Sergei V Novikov<sup>2</sup> and C Thomas Foxon<sup>2</sup>

<sup>1</sup> HH Wills Physics Laboratory, University of Bristol, Tyndall Avenue, Bristol, BS2 1TL, UK

<sup>2</sup> School of Physics and Astronomy, University of Nottingham, Nottingham NG7 2RD, UK

Received ZZZ, revised ZZZ, accepted ZZZ

Published online ZZZ (Dates will be provided by the publisher.)

**Keywords** InGaN nanorods, Solar Cells, MBE, TEM

\* Corresponding author: e-mail: richard.webster@bristol.ac.uk, Phone: +44179288750

This paper demonstrates the growth of InGaN nanorods and lateral growth over nanorod arrays using molecular beam epitaxy. It is shown that nitrogen rich growth conditions result in a nanorod array and that, by changing to metal rich conditions, lateral growth may be enhanced to coalesce the nanorods into a continuous overgrown film. Energy dispersive x-ray spectroscopy has been used to demonstrate that the nanorods

display a core-shell structure with In-rich cores and In-poor edges. Transmission Electron Microscopy has shown that the nanorods are free of dislocations. However when lateral growth occurs basal plane stacking faults are generated. It is shown that this stacking fault generation leads to a change in structure from hexagonal to cubic. When coalescence has occurred large angle grain boundaries are present.

Copyright line will be provided by the publisher

**1 Introduction** Indium Gallium Nitride ( $\text{In}_x\text{Ga}_{1-x}\text{N}$ ) has a direct band gap of 0.7eV ( $x=1$ ) to 3.4eV ( $x=0$ ). This spans the visible spectrum and makes InGaN a viable candidate for optoelectronic devices such as LEDs, lasers and photovoltaics [1, 2]. Growth of InGaN may be achieved using various growth techniques such as molecular beam epitaxy (MBE) [3, 4], pulsed laser deposition [5] and metal-organic chemical vapour deposition [2, 6, 7]. However due to a lack of adequately lattice matched substrates InGaN films generally have high threading dislocations.

There are also issues associated with indium incorporation during growth, leading to spatial variations in In content, especially in In rich films [8]. Work by Kehagias et al [9] has used EDX mapping to show that InGaN nanorods grown on (111)-Si substrates have increasing In composition along the length of nanorods which is due to high In desorption rates at temperatures of 450°C. In segregation has also been reported in quantum well and quantum dot structures [4] and in other alloy systems such as InGaAs [10].

InGaN usually has the hexagonal wurtzite form which has a stacking sequence ..ABABAB.. but may also exist in the cubic zinc-blende phase which has the ..ABCABC..

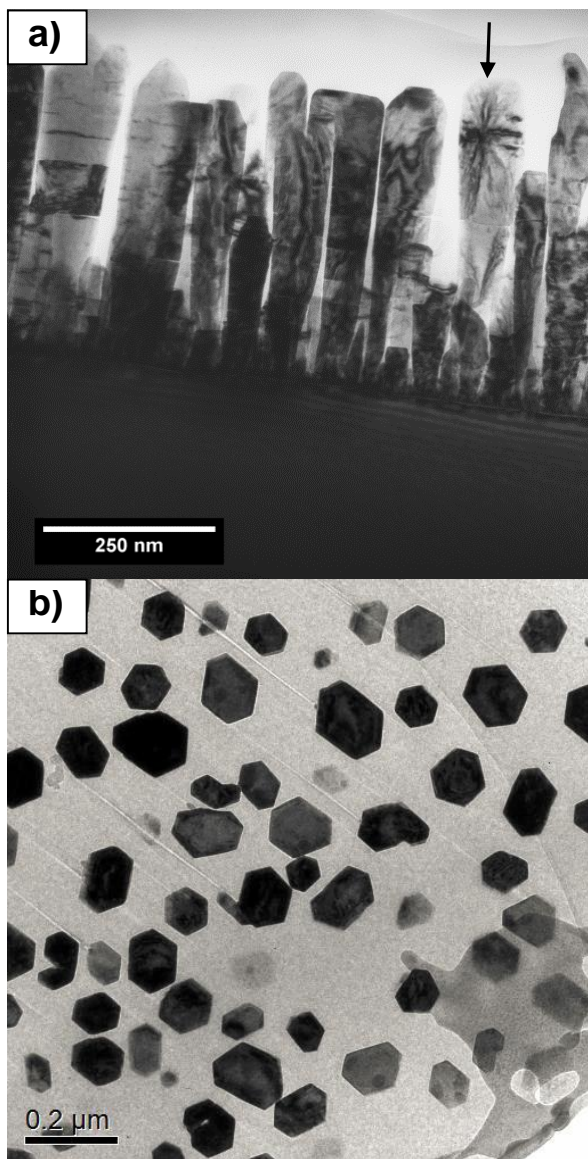
stacking sequence. The wurtzite form is polar in the  $c$ -direction (0002), which creates spontaneous electric piezoelectric fields [11] which may act to separate electron hole pairs which is ideal for a photovoltaic device. The zinc-blende structure is not polar [12, 13] and so lacks the piezoelectric field, much like non-polar orientations of wurtzite material which make these favourable to LED and Laser devices.

Previous work with GaN on sapphire [14] has shown that by controlling the N:Ga ratio to N-rich conditions, growth of GaN nanorods with little to no threading dislocations in the nanorods may be achieved. Furthermore by subsequently changing the growth conditions to Ga-rich a GaN film may be grown over the nanorod array which had a low dislocation density,  $\approx 10^8\text{cm}^{-2}$ .

**2 Method** Growth of the samples presented in this paper was performed at Nottingham University by MBE. Samples of InGaN have been directly grown on Si in a Varian ModGen II system at growth temperatures of 400°C to 500°C. Nitrogen-rich conditions were used to promote vertical growth whilst metal-rich conditions were used for lateral growth.

Copyright line will be provided by the publisher

1 All cross section samples were prepared for TEM by  
 2 mechanically polishing to 100 $\mu\text{m}$  and ion thinning using a  
 3 Gatan PIPS Ar ion thinner. Samples were thinned at 5keV  
 4 until perforation, then at 3keV to remove surface damage.  
 5 Plan view TEM samples have been prepared using a FEI  
 6 DualBeam FIB/SEM which uses Ga ions accelerated at  
 7 15kV for the initial sectioning and a lower energy 3kV  
 8 beam to reduce the damage caused by the Ga ion beam. To  
 9 make the plan view section the sample was first encased in  
 10 epoxy resin, which provides support for the nanorods  
 11 during and after milling. The specimen was then mounted  
 12 with the InGaN/Si interface normal to the focused gallium  
 13 ion beam direction and a lamella cut out.



14  
15  
16  
17  
18  
19  
20  
21  
22  
23  
24  
25  
26  
27  
28  
29  
30  
31  
32  
33  
34  
35  
36  
37  
38  
39  
40  
41  
42  
43  
44  
45  
46  
47  
48  
49  
50  
51  
52  
53  
54  
55  
56  
57  
**Figure 1** TEM of an N-rich growth resulting in InGaN nanorods shown in a) mechanically polished cross-section with bend contours along the c-direction (arrowed) and b) plan-view prepared by FIB milling.

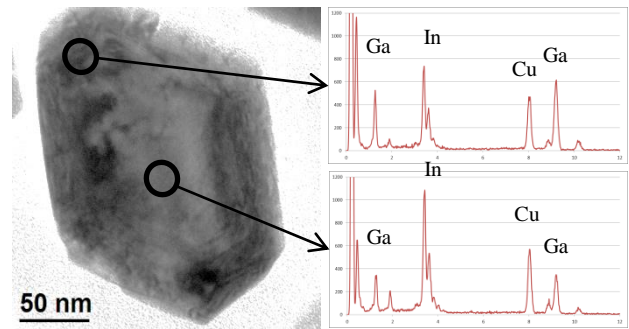


**Figure 2** EDX spectra taken from nanorod in plan view. The spectra are from the regions indicated and show a significant increase of In at the centre of the nanorod when compared with the edge.

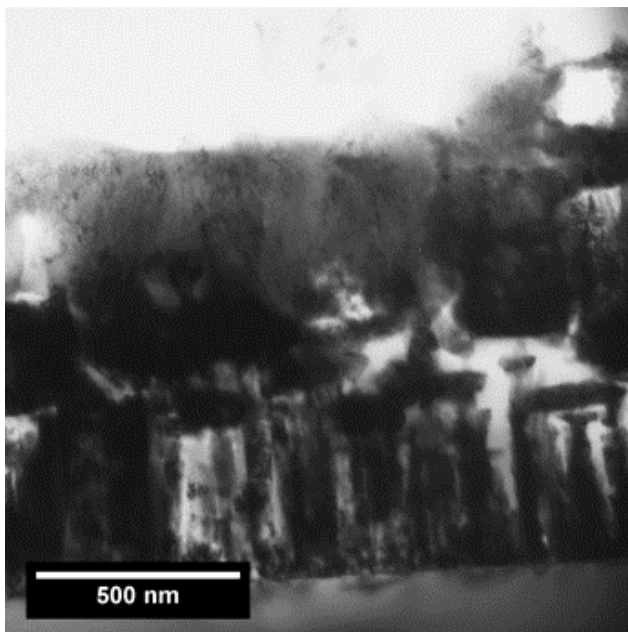
TEM was performed on a Philips EM430 operated at 200kV. Energy dispersive X-ray spectroscopy was performed on a JEOL 2010 operated at 160kV equipped with an Oxford Instruments EDX spectrometer which was used to characterise the composition of the nanorods by taking point spectra with a spot with a diameter of 20nm.

**3 Results and Interpretation** Figure 1 shows TEM of InGaN structures grown on (111)-silicon in N-rich conditions at a temperature of 400°C. This promotes vertical growth and suppresses lateral growth. These nanorods are ~500nm long and 100nm wide, are faceted with the c-axis perpendicular to the substrate and are free of threading dislocations. Arrowed in Figure 1(a) is a nanorod orientated close to the  $[11\bar{2}0]$  zone axis, which shows contours along the length of the nanorod indicating that the nanorod is bending around the c-axis. These contours are not visible in all nanorods as there is significant rotation about the c-axis as can be seen in Figure 1(b). This demonstrates that nanorods have not grown epitaxially.

Plan view of the nanorods shown in Figure 1(b) demonstrates the faceted nature of the nanorods. Spot EDX has been taken on this sample (shown in Figure 2) with the electron beam at the edges of the structures and at the centres and has shown a significant increase of In composition towards the centre of the nanorods which explains the bending around the c-axis (seen in Figure 1(a)) due to the larger lattice constant of the indium rich core.

Figure 3 shows a sample grown in metal-rich conditions and at a higher temperature of 500°C. In these conditions the lateral growth is enhanced and a film has grown over the nanorod array. The grain size of the overgrown film is larger than 500nm which spans multiple nanorods implying that as neighbouring nanorods coalesce there is a degree of recrystallisation. There are large angle grain boundaries where large misorientated grains

1 coalesce. When coalescence is attempted at a lower growth  
 2 temperature (400°C) as shown in Figure 4, stacking faults  
 3 are observed where the growth conditions have been  
 4 changed. There is also a change in structure from  
 5 hexagonal in the nanorods to cubic during lateral growth  
 6 which can be seen in the selected area diffraction (SAD)  
 7 pattern of Figure 4(c) which shows the [110] zone axis  
 8 diffraction pattern for the cubic zinc-blende phase. After  
 9 a second stacking fault, inclined 70° to the basal plane,  
 10 the structure reverts to the wurtzite structure as shown by the  
 11 [11 $\bar{2}$ 0] zone axis SAD pattern of Figure 4(d). EDX has  
 12 shown that the composition of the cubic area is  
 13 significantly more In-rich when compared to the hexagonal  
 14 areas.



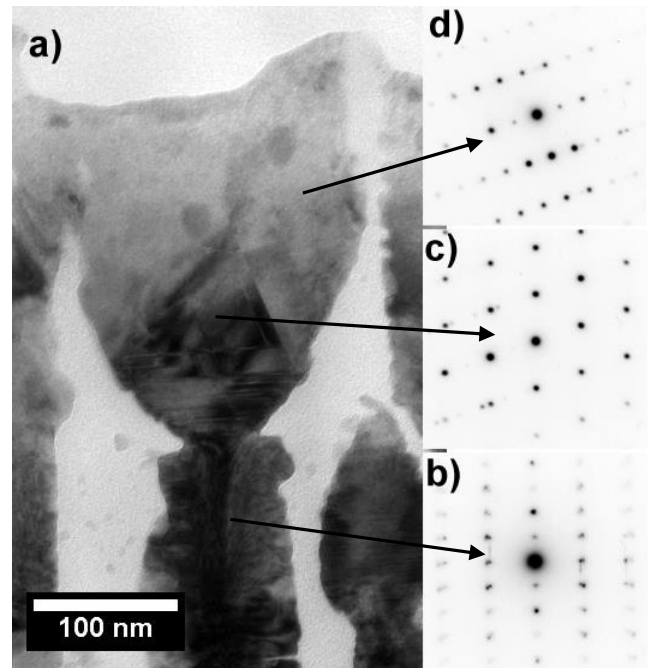
15  
16  
17  
18  
19  
20  
21  
22  
23  
24  
25  
26  
27  
28  
29  
30  
31  
32  
33  
34  
35  
36  
37  
38 **Figure 3** A N-rich growth resulting in nanorods at the base,  
 39 followed by a metal rich growth which resulted in coalescence.

40  
41  
42  
43  
44  
45  
46  
47  
48  
49  
50  
51  
52  
53  
54  
55  
56  
57  
**4 Discussion** These results demonstrate that by  
 controlling the growth conditions defect free nanorods may  
 be directly grown on silicon. It is possible to achieve  
 coalescence of these structures using metal-rich conditions  
 resulting in grains which span multiple nanorods, typically  
 wider than 1 $\mu$ m. It may be seen when observing the  
 nanorod array in plan-view (Figure 1(b)) that the nanorods  
 are rotated with respect to each other around the c-axis.  
 This leads to the large angle grain boundaries observed  
 where coalescence occurs.

EDX has been used to show there are large variations  
 in composition radially in the nanorods. The change in  
 composition leads to mismatch strains with the In-poor  
 shell being under tension. This can explain the bending  
 observed occasionally along the nanorod axis as partially  
 thinned nanorods relax (Figure 1(a)). The radial variation  
 in composition may be explained by considering  
 desorption and migration of In. At growth temperatures of

400-500°C, any Ga deposited should be essentially  
 immobile and not desorbed. The core-shell structure may  
 be explained by considering In desorption at the growth  
 temperature, this acts to shield nanorods from the In source  
 during growth resulting in an In-poor surface.

A change to metal-rich growth conditions has the  
 effect of increasing the In composition rapidly. This causes  
 an in-plane stress which explains the large number of  
 stacking faults in this transition region as stacking faults  
 can relieve strain in the basal plane. The change of  
 structure from hexagonal in the nanorods to cubic in the  
 lateral growth might be caused by the local change in the  
 stacking sequence from hexagonal to cubic associated with  
 a stacking fault. In cubic material, a stacking fault is  
 associated with a local transition from cubic to hexagonal  
 stacking, and it may be that this accounts for the reverse  
 transition from cubic to hexagonal material after the stress  
 caused by the change in composition has been  
 accommodated.



39  
40  
41  
42  
43  
44  
45  
46  
47  
48  
49  
50  
51  
52  
53  
54  
55  
56  
57  
**Figure 4** a) Cross section TEM of a nanorod with subsequent  
 metal-rich growth with a large number of stacking faults at the  
 interface of the two growth conditions. SAD from the regions  
 arrowed show a change of structure from hexagonal to cubic and  
 back to hexagonal in b), c) and d) respectively. b) and d) are  
 hexagonal [11 $\bar{2}$ 0] zone axis diffraction patterns and c) is a cubic  
 [110] diffraction pattern. The central nanorod is in the [11 $\bar{2}$ 0]  
 orientation.

**5 Summary** It has been demonstrated that InGaN  
 nanorods may be grown by MBE with N-rich conditions,  
 which is in agreement with previous work on GaN. There  
 is a higher indium content in the centre of the nanorods  
 which has been shown by EDX. It has also been  
 demonstrated that it is possible to coalesce nanorods using

1 metal-rich conditions which tends to form a continuous  
2 layer. For low growth temperatures in metal-rich  
3 conditions, stacking faults occurred which had the effect of  
4 changing the structure from hexagonal to cubic, this was  
5 reversible, resulting in inclined hexagonal growths.  
6

7 **Acknowledgements** The authors would like to  
8 acknowledge funding from EPSRC (Grant number EP/I035501/1)  
9

## 10 **References**

- 11 [1] T. Kuykendall, P. Ulrich, S. Aloni, and P. Lang, *Nature*  
12 *Mater.* **6**, 951 (2007).  
13 [2] O. Jani, I. Ferguson, C. Honsberg and S. Kurtz, *Appl. Phys.*  
14 *Lett.*, **91**, 261108 (2007).  
15 [3] S. Albert, B. A. S. M, X. Kong, A. Trampert, and E. Calleja,  
16 *Nanotechnology*, **24**, 175303 (2013).  
17 [4] V. Lemos, E. Silveira, J. R. Leite, A. Tabata, R. Trentin, L.  
18 M. R. Scolfaro, T. Frey, D. J. As, D. Schikora, and K.  
19 Lischka, *Phys. Rev. Lett.*, **84**, 3666 (2000).  
20 [5] T. Wang, S. Ou, K. Shen, and D. Wu, *Opt. express*, **21**,  
21 7337 (2013).  
22 [6] Y. Ra, R. Navamathavan, J. Park, and C. Lee, *ACS applied*  
23 *materials & interfaces* **5**, 2111 (2013).  
24 [7] C. J. Neufeld, N. G. Toledo, S. C. Cruz, M. Iza, S. P.  
25 DenBaars, and U. K. Mishra *Appl. Phys. Lett.*, **93** 143502  
26 (2008).  
27 [8] F. A. Ponce, S. Srinivasan, A. Bell, L. Geng, R. Liu, M.  
28 Stevens, J. Cai, H. Omiya, H. Marui, and S. Tanaka, *Phys.*  
29 *Status Solidi (b)* **240**, 273 (2003).  
30 [9] T. Kehagias, *Physica E* **42**, 2197 (2010).  
31 [10] S. Martini, A. A. Quivy, M. J. da Silva, T. E. Lamas, E. C. F.  
32 da Silva, J. R. Leite, and E. Abramof, *J. Appl. Phys.*, **94**,  
33 7050 (2003).  
34 [11] D. Cherns, J. Barnard, and F. Ponce, *Solid State Commun*  
35 **111**, 281 (1999).  
36 [12] K. Lischka, *J. Cryst. Growth*, **231**, 415 (2001).  
37 [13] O. Ambacher, J. Majewski, C. Miskys, A. Link, M.  
38 Hermann, M. Eickho\_, M. Stutzmann, F. Bernardini, V.  
39 Fiorentini, V. Tilak, B. Schaff, and L. F. Eastman, *J. Phys.:*  
40 *Condens. Matter*, **14**, 3399 (2002).  
41 [14] D. Cherns, L. Meshi, I. Griffiths, S. Khongphetsak, S. V.  
42 Novikov, N. Farley, R. P. Champion, and C. T. Foxon, *Appl.*  
43 *Phys. Lett.*, **92**, 121902 (2008).  
44  
45  
46  
47  
48  
49  
50  
51  
52  
53  
54  
55  
56  
57